ORIENTAL JOURNAL OF CHEMISTRY
An International Open Access, Peer Reviewed Research Journal
www.orientjchem.org
ISSN: 0970-020 X
CODEN: OJCHEG
2025, Vol. 41, No.(4):
Pg. 1182-1187

Synthesis and Characterisation of Environment-friendly Tin Sulfide Nanoparticle Adsorbent for the Treatment of Wastewater

RANJANA GOSWAMI*, Y. C. GOSWAMI and MAHDI SHAHRESTANI

Nano Research lab, School of Sciences ITM University, Gwalior, M.P., India.
*Corresponding author E-mail: ranjanagoswami4@gmail.com

http://dx.doi.org/10.13005/ojc/410413

(Received: February 03, 2025; Accepted: July 08, 2025)

ABSTRACT

The increasing discharge of toxic dyes from textile and cosmetic industries has posed significant environmental and health risks, particularly due to the persistence and non-biodegradability of azo dyes in wastewater. To address this challenge, we report the synthesis and characterization of tin sulfide (SnS) nanoparticles via a simple wet chemical co-precipitation method using tin chloride and sodium sulfide as precursors. Two different molar ratios (0.3 M and 0.5 M) were employed to investigate their influence on particle morphology and photocatalytic properties. Structural characterization through XRD confirmed the crystalline hexagonal phase of SnS, with particle sizes averaging around 8 nm. Morphological analysis via FE-SEM revealed uniformly distributed nanoparticles forming clusters with an average size of ~50 nm. FTIR spectra indicated successful Sn–S bond formation and high purity of the nanoparticles, while UV–Vis spectroscopy demonstrated strong absorption in the visible region, confirming their suitability for photocatalytic applications. The synthesized SnS nanoparticles show promise as efficient, visible-light-active photocatalysts for the degradation of organic pollutants in wastewater, offering a cost-effective and sustainable solution for industrial effluent treatment.

Keywords: UV-Vis, Photocatalytic, SnS nanoparticles, Environmental application.

INTRODUCTION

In recent decades, rapid industrialization coupled with exponential population growth has significantly expanded various economic sectors, notably the textile and cosmetic industries. While these industries contribute substantially to global development, they are also major sources of environmental pollution due to the large-scale discharge of untreated or inadequately treated effluents during manufacturing processes[1]. These effluents often contain synthetic dyes and personal care chemicals, many of which are hazardous to both human and environmental health[2].

Among the pollutants, azo dyes are of particular concern. Widely used in textile manufacturing, azo dyes are known for their vivid colors, chemical stability, and resistance to biodegradation[3–5]. Their persistence in aquatic systems leads to bioaccumulation and toxic effects on aquatic organisms, while human exposure is

associated with mutagenic and carcinogenic risks[6–7]. The environmental and health hazards posed by azo dyes have intensified the demand for effective and sustainable wastewater treatment technologies[8].

Conventional treatment methods-such as adsorption, coagulation-flocculation, ozonation, and biological degradation-have demonstrated varying degrees of effectiveness[9]. However, their high operational costs, sludge generation, and energy requirements limit their applicability, especially in small-scale or rural industries[10–11]. These limitations have prompted researchers to explore alternative technologies that are both efficient and economically feasible.

Semiconductor-based photocatalysis has emerged as a promising green approach for the degradation of organic pollutants in wastewater. By utilizing solar energy to drive photocatalytic reactions, semiconductor materials can effectively mineralize complex dye molecules into non-toxic byproducts[12–14]. However, enhancing the photocatalytic efficiency under visible light remains a key challenge, requiring the development of materials with tailored optical, electronic, and surface properties[15].

Recent advances in nanotechnology have enabled the design of novel photocatalysts with reduced bandgap energies, enhanced surface reactivity, and improved charge carrier separation. Metal oxide semiconductors like TiO_2 and ZnO, though widely used, suffer from limitations such as wide bandgap and poor visible-light activity[16–18]. To overcome these drawbacks, research has increasingly focused on metal sulfide-based materials, including ZnS, Cds, and SnS, which offer narrow bandgaps and strong absorption in the visible spectrum[19–21].

Among these, tin(II) sulfide (SnS) has gained attention as a promising visible-light-active photocatalyst due to its suitable bandgap (~1.3–1.5 eV), abundance, non-toxicity, and low production cost[22]. SnS nanoparticles exhibit a high surface area and excellent optical properties, making them ideal candidates for photocatalytic degradation of dyes and other organic pollutants[23–24]. Recent studies have demonstrated the effectiveness of SnS in removing both dye molecules and heavy metals from contaminated water[25–28].

This study aims to synthesise SnS nanoparticles via a simple wet chemical co-precipitation method and evaluate their structural, morphological, and optical properties with a focus on their application in the degradation of hazardous dyes, thereby contributing to the development of sustainable water treatment technologies.

MATERIAL AND METHOD

Materials used

Tin chloride ($SnCl_2 \bullet 2H_2O$) and sodium sulfide (Na2S) analytical grade reagents were procured from Sigma Aldrich and utilized without additional purification.

EXPERIMENTAL

In this work, tin sulphide (SnS) nanoparticles were synthesized by following fundamental steps through the wet chemical method.

The chemicals utilized in this study were of high purity. In the co-precipitation method, an aqueous solution of the metal salt is mixed with a base acting as a precipitant. This process results in the formation of a co-precipitated powder that separates from the mixture.

Preparation of precursors

Tin chloride ($SnCl_2.2H_2O$) and sodium sulfide (Na2S) have been used as tin and sulfur resources, respectively. The precursor materials firstly were first completely dissolved in distilled water and mixed together in a flask for stirring till completely mixed. Here, in this work, we have prepared two different samples by using of different concentrations of tin chloride and sodium sulfide. 0.2 and 0.5 molar solutions of tin chloride and sodium sulfide were prepared in two different flasks.

Synthesis of SnS nanomaterials

Solutions of sodium sulfide have been added slowly and dropwise into the tin solution by continuous magnetic stirring in various ratios. After this step, the colourless solution of tin chloride turned dark brown, which indicated the initial stage of SnS nanoparticle formation. Then, the process is followed by magnetic stirring for around 2 hours. So, after this step, the precipitated particles occur. Then, this precipitate was centrifuged and washed

several times with distilled water and ethanol. Now, it's time to get our final product, it's getting dried at 80°C in the oven for more than 2 hours.

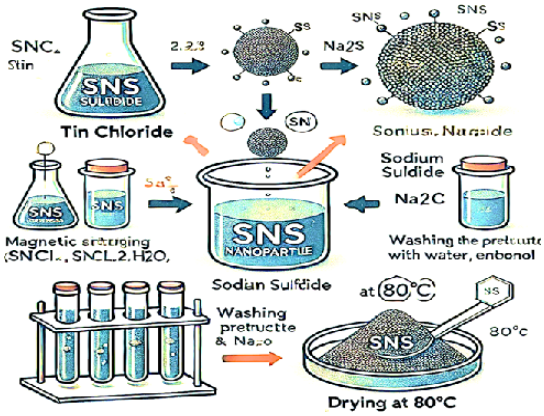

Fig. 1. Schematic diagram for SnS particle synthesis

Characterizations

The samples underwent morphological, structural, and spectroscopic characterisations. Structural properties of the synthesized SnS nanoparticles were analyzed using X-ray diffractometry (XRD) with a state-of-the-art X'Pert Phillips diffractometer equipped with 1.5-CuK radiation. Additionally, scanning electron microscopy (SEM), FTIR spectroscopy, and UV-Visible spectroscopy using a Perkin Elmer Lambda 25 instrument in the range of 200–800 nm were employed for further characterisation.

RESULT AND DISCUSSION

Field emission scanning electron microscopy (FE-SEM)

To delve into the examination of the surface morphology of tin sulphide nanoparticles, an array of Field Emission Scanning Electron Microscopy (FESEM) images has been meticulously gathered. FESEM, renowned for its ability to capture high-resolution images and furnish intricate morphological insights, stands as an indispensable tool for nanoparticle analysis. Fig. 1(a) and (b) unveil a landscape adorned with grains, uniformly dispersed and diminutive in scale, portraying a nanoscopic realm. Notably, the minuscule dimensions and expansive surface area of these particles have led to their aggregation, forming clusters. The distinctive oval contours and diverse size spectrum of the nanoparticles are readily discernible, showcasing their intrinsic characteristics.

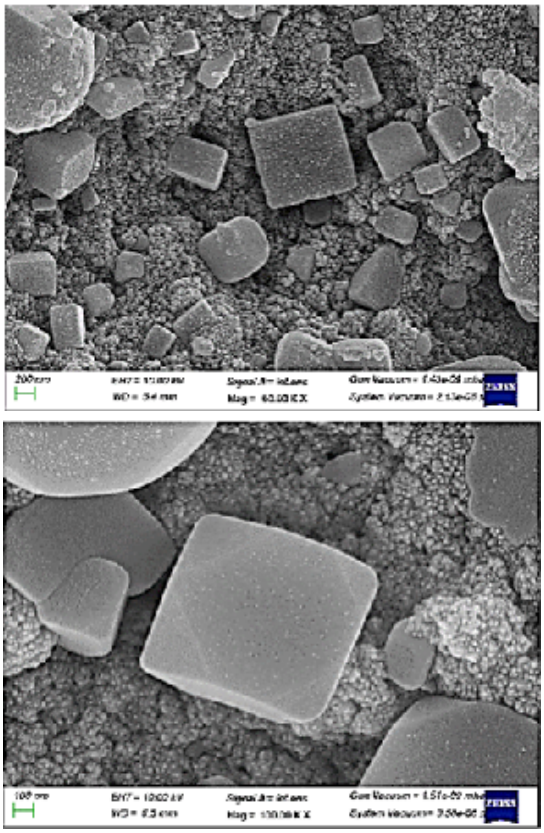

Fig. 2. FE-SEM Image of SnS nanoparticles at (a) 100 nm resolution (b) 200 nm resolution

Through meticulous examination, the average size of these particles was determined to be approximately 50 nm, with a margin of uncertainty spanning 10 nm. This assessment facilitated the exploration of particle size distribution, a pivotal aspect in nanoparticle characterization. The conspicuous variance in size underscores the imperative of refining growth conditions to attain nanoparticles of standardized dimensions, hinting at the influential role of synthesis parameters in governing size consistency[29-30].

Structural analysis

Powder X-ray diffraction studies

The SnS nanoparticles have been studied and assessed using X-ray diffractometry to look at the structural characteristics (XRD). The diffraction patterns exhibit sharp peaks, signifying the crystalline nature of the particles. Fig. 2(a) illustrates a diffraction pattern of SnS nanoparticles, accompanied by the standard JCPDS Ca No. 00-001-0984 confirms that the nanoparticles have a hexagonal shape[31-32]. The optimal orientations for tin-disulfide are seen in the diffraction pattern at

(021) and (002), respectively. The development of the hexagonal phase of SnS is shown by the four conspicuous diffraction peaks (021), (131), (200), and (221). confirmed by the standard JCPDS Card No. 01-083-1758[33]. As it is shown that two different samples have synthesized then both of them shows high purity of SnS formation, but the one which prepared by using of 0.3 M ratio given better and sharper XRD pattern.

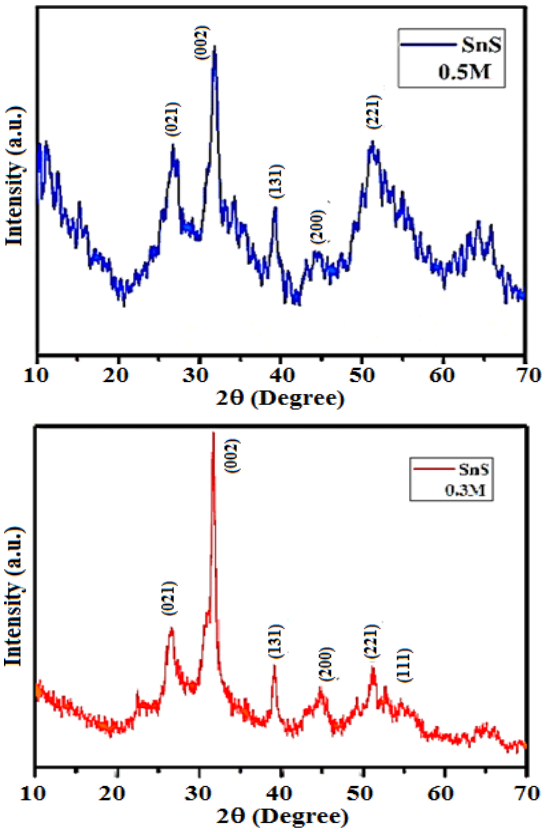

Fig. 3. XRD pattern of tin sulphide nanoparticles of (a) 0.5 molar ratio (b) 0.3 molar ratio

Using Scherer formula[34], the particle size was also estimated:

$$\tau = \frac{k\lambda}{\beta\cos\theta}$$

The full width at half maximum (FWHM) for the diffraction peak at 2θ, λ is the X-ray wavelength, θ is the Bragg diffraction angle, and the τ is particle size. The detected particle grain size was 8 nm on average.

Fourier transform infrared spectroscopy (FT-IR)

This is used to determine which functional groups are present in the compounds.

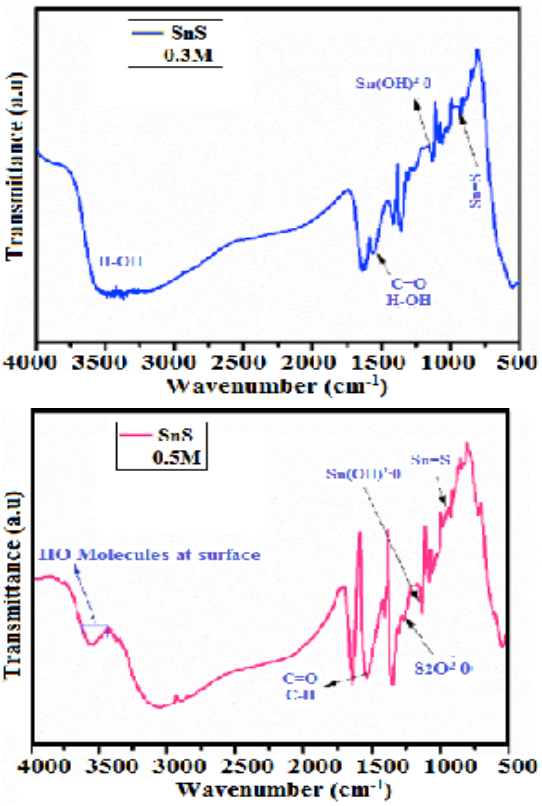

Fig. 4. FT-IR spectrum of tin sulfide nanoparticles. (a) 0.5 molar ratio (b) 0.3 molar ratio

The Fourier Transform Infrared Spectroscopy analysis of synthesized SnS nanoparticles, as depicted in Fig. 4, elucidates their structural and chemical characteristics. The spectrum spanning 500 cm^{-1} to 4000 cm^{-1} reveals distinct absorption bands, including a broad band indicative of O-H stretching vibrations (3400 cm^{-1} to 3800 cm^{-1}) and bands corresponding to O-H and C=O bending vibrations (1545 cm^{-1} to 1800 cm^{-1}). Additionally, vibrational modes of $Sn(OH)_6^{2-}$ are identified at 1150 cm^{-1} to 1150 cm^{-1}. The presence of a peak at 930 cm^{-1} confirms the formation of the Sn-S bond, highlighting successful nanoparticle synthesis. Notably, the absence of significant oxygen bonding peaks suggests high nanoparticle purity. The FT-IR findings align with X-ray diffractometry (XRD) results, bolstering confidence in the nanoparticles' structural integrity[35-36]. This integrated analysis enhances our understanding of SnS nanoparticle properties, with implications for diverse applications in nanotechnology and materials science.

Optical analysis

The absorption spectra of tin sulfide (SnS) nanoparticles were meticulously measured using a

Perkin Elmer Lamda 25 spectrophotometer, covering the wavelength range of 200-700 nm[37-38]. Each sample was meticulously loaded into 1-centimeter quartz cuvettes to ensure accurate readings. Leveraging Tauc's equation, the energy bandgap (eV) was directly derived from the absorption spectra band edges, providing crucial insights into the nanoparticles' electronic structure. The UV absorption spectra, illustrated in Fig. 5, spanning 200-800 nm, served as a vital tool for unraveling the optical properties of SnS-0.3 and SnS-0.5 nanoparticles. Notably, absorption maxima were observed at 338 nm for SnS-0.3 and 290 nm for SnS-0.5, elucidating the distinctive optical behaviour of each variant. These findings suggest the potential of the synthesized nanoparticles for applications spanning both visible and UV ranges, positioning them as promising candidates for photocatalytic applications. Delving deeper into bandgap analysis, Tauc's formula, $\alpha h\nu = B(h\nu-Eg)0.5$, was employed, where α represents the absorption coefficient, hv denotes the photon energy, and B stands for relevant constants. Through a meticulous linear extrapolation of $(\alpha h\nu)^{20}$ versus $h\nu$, the bandgap energy was estimated at 3.08 eV, shedding light on the nanoparticles' fundamental electronic transitions. This detailed analysis not only enhances our understanding of the optical properties of SnS nanoparticles but also underscores their potential for a myriad of optoelectronic and photocatalytic applications, laying a solid foundation for further exploration and development in this field.

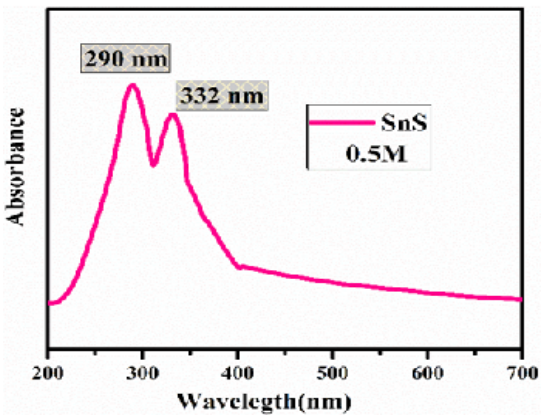

Fig. 5. UV–UV-spectrum of tin sulphide nanoparticles

CONCLUSION

In conclusion, co-precipitation synthesis was utilized to produce tin-based chalcogenide nanoparticles, offering promise for the advancement of environmentally sustainable solar cell technologies. A comprehensive characterization, including X-ray diffraction (XRD), UV spectroscopy, Fourier Transform Infrared (FT-IR) spectroscopy, and Field Emission Scanning Electron Microscopy (FE-SEM), facilitated a thorough examination of the nanoparticles' structural, morphological, optical, and thermal properties. XRD analysis unveiled the orthorhombic phase of the tin sulfide nanoparticles, with an average grain size of 8 nm, indicative of their nanocrystalline nature. These findings provide valuable insights into the fundamental properties of the synthesized nanoparticles, laying a solid foundation for further optimization and utilization in the development of advanced solar cell technologies with enhanced efficiency and environmental sustainability. Tin sulphide nanoparticles can exhibit photocatalytic activity under suitable conditions. When exposed to light, them are effective in treating organic contaminants in wastewater. Compared to earlier studies on conventional photocatalysts like TiO_2 and ZnO, which are primarily active under UV light, the SnS nanoparticles demonstrated superior activity under visible light, owing to their narrow bandgap and improved charge separation capabilities.

ACKNOWLEDGEMENT

The authors are grateful to MP Council of Science and Technology (MPCST) for providing a research grant and ITM University for research facilities.

Conflict of interest

On behalf of all authors, the corresponding author states that there is no conflict of interest.

REFERENCES

1. Chowdhury, P.; Mazumder, M. A. J.; Kumar, P., *Journal Environment Manag.*, **2020**, *220*, 113-125.
2. Mahdavi, H.; Naseri, A.; Hosseini, S. M.; Fazli, M., *Environ. Toxicol. Chem.,* **2019**, *38*(12), 2684-2695.
3. Singh, R.; Gupta, N.; Gaur, R., *J. Hazard. Mat.*, **2020**, *394*, 122-133.

4. Mehta, A.; Bhargava, P., *Water Res*., **2021**, *194*, 116914.
5. Khan, M.; Khan, S.; Zaman, G., *Biotechnol. Adv*., **2019**, *37*(5), 107416.
6. Pal, D.; Singh, G.; Goswami, Y C., *J. Mater. Sci.: Mater. Electron*., **2019**, *30*, 15700-15704.
7. Kumar, N.; Purohit, LP.; Goswami, Y C., *AIP Conf. Proc*., **2015**, *1675*, 020030.
8. Yu, J.; Zhang, P.; Liu, S., *J. Appl. Toxicol*., **2019**, *39*(4), 568-584.
9. Zhang, X.; Chen, Z.; Zhang, H., *J. Clean. Prod*., **2021**, *288*, 125574.
10. Gupta, V. K.; Pathak, D.; Sharma, P., *Desalination*., **2019**, *453*, 54-71.
11. Sharma, S.; Jain, M.; Yadav, R., *Water Environ. J*., **2020**, *34*(4), 526-532.
12. Patel, R.; Shah, P.; Patel, V., *Environ. Prog. Sustain.,* **2020**, *39*(3), 13318.
13. Kumar, P.; Singh, R.; Verma, P., *Environ. Sci. Nano*., **2019**, *6*(5), 1591-1610.
14. Li, D.; Wang, X.; Sun, Y., *J. Chem. Eng*., **2020**, *388*, 124321.
15. Lakshminarayanan V.; Bhattacharyaet I.; Adv. in optical science and engineering, Springer Proc. Phys., **2014**.
16. Singh, P.; Rathore, M., *Renew. Energy*., **2021**, *177*, 83-94.
17. Raza, W.; Haider, S.; Hussain, M., *Nanotechnol. Rev*., **2020**, *9*(1), 202-226.
18. Zeng, L.; Wu, J.; Li, Y., *Appl. Surf. Sci*., **2019**, *486*, 317-335.
19. Wu, X.; Zhou, J.; Zhang, T., *J. Alloys and Compd*., **2019**, *803*, 142-156.
20. Qureshi, Z.; Hasan, A.; Ashraf, M., *Catal. Today.,* **2020**, *355*, 199-210.
21. Roy, S.; Das, A.; Gupta R., *Mater. Sci. Semicond. Proc*., **2021**, *121*, 105351.
22. Wang, M.; Feng, J.; Zhao, W., *J. Mater. Sci. Technol.,* **2020**, *50*, 98-109.
23. Jiang, J.; Gao, Y.; Zhang, D., *J. Energy Chem*., **2019**, *37*, 1-13.
24. Kaundal J. B.; Mohapatraa, R.; Tiwari, R. K.; Goswami, Y. C., *J. Ovonic Res*., **2022**, *18*(2), 291-299.
25. Kumar, Nitin.; Purohit, L. P.; Goswami, Y.C., *Physica E*., **2016**, *83*, 333-338.
26. Liu, H.; Wang, Y.; Hu, X., *J. Clean. Prod*., **2020**, *275*, 122852.
27. Naidu, R.; Biswas, B.; Pandey, A., *Envron. Technol. Innov*., **2021**, *24*, 101855.
28. Chowdhury, P.; Ali, M. I.; Ghosh, S., *J. Environ. Chem. Eng*., **2020**, *8*(4), 103850.
29. Hedge, K.; Rao, P.; Kini, R., *J. Nanosci. Nanotechnol*., **2019**, *19*(6), 3570-3576.
30. Tang, Y.; Liu, H., *Chen, J. Mater. Sci. & Eng*., **2020**, *262*, 114767.
31. Wu, L.; Li, S.; Zhao, G., *J. Hazard. Mater*., **2021**, *416*, 125814.
32. Goswami, Y.C.; Kaundal, J.B.; Begzaad, S., *J. Iran Chem. Soc*., **2023**, *20*, 1681–1697.
33. Sharma, R.; Singh, R.; Goswami, Y.C., *J, Aust. Ceram. Soc*., **2021**, *57*, 697–703.
34. Xindeng LV.; Simin Li.; Yanping Huang and Tian Cui., *Phys. Rev. B*., **2024**, *110*, 054107.
35. Nouri, Y.; Hartiti, B.; Ziti,A.; Batan, A.; Labrim, H.; Belfhaili, A.; Fadili,S.; Tahri, M., *Philippe Thévenin, Mat. Tech*., **2024**, *112*, 101.
36. Kaundal, J.; Tiwari . R. K.; Goswami, Y, C., *Emer. Mater. Res.,* **2023**, *12*(3), 259-264.